Summary: We have prepared hexa-*p*-phenylene based rod-coil molecules with identical coil volume fractions, but different poly(propylene oxide) (PPO) coil architectures (linear versus dibranched), and investigated their self-assembling behavior in the solid state by small angle X-ray scattering (SAXS) and transmission electron microscopy (TEM) techniques. Rod-coil molecules with a linear PPO coil showed a honeycomb-like lamellar assembly of rod segments with hexagonally arrayed PPO coil perforations. In contrast, the rod-coil molecules with dibranched PPO coils self-organized into rod bundles with a body centered tetragonal symmetry surrounded by a PPO coil matrix. These results demonstrate that the steric hindrance at the rod/coil interface arising from coil architectural variation is a dominant parameter governing supramolecular rod assembly in the rod-coil system.

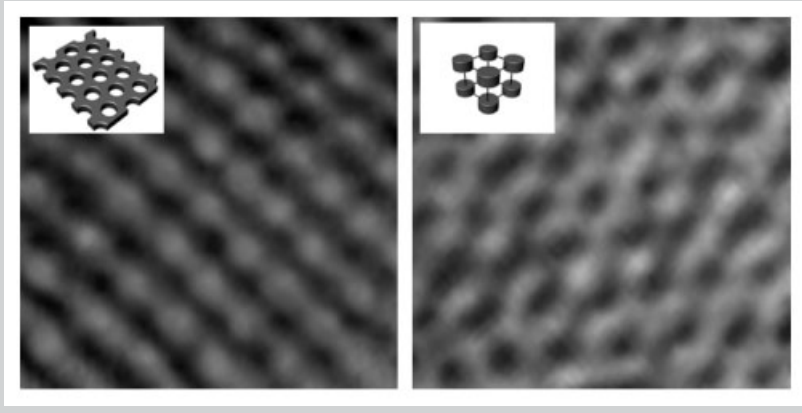

TEM images and schematic illustrations of the self-assembled structures of rod-coil molecules with linear (left) and dibranched (right) PPO coils, respectively.

Chain Architecture Dependent 3-Dimensional Supramolecular Assembly of Rod-Coil Molecules with a Conjugated Hexa-*p*-phenylene Rod

Myoung-Hwan Park,[1] *Ja-Hyoung Ryu,*[1] *Eunji Lee,*[1] *Kyung-Hee Han,*[2] *Yeon-Wook Chung,*[2] *Byoung-Ki Cho,**[2] *Myongsoo Lee**[1]

[1] Center for Supramolecular Nano-Assembly and Department of Chemistry, Yonsei University, Seoul, 120–749, Korea
E-mail: mslee@yonsei.ac.kr
[2] Department of Chemistry and Institute of Nanosensor and Biotechnology, Dankook University, 147, Hannam-ro, Yongsan-gu, Seoul 140–714, Korea
E-mail: chobk@dankook.ac.kr

Received: June 28, 2006; Accepted: July 28, 2006; DOI: 10.1002/marc.200600445

Keywords: body centered tetragonal micellar structure; honeycomb-like lamellar structure; rod-coil molecules; self-assembly; supramolecular structures

Introduction

Rod-coil molecules consist of two conformationally distinct blocks such as a rigid rod and a flexible coil. They are considered to be a different class of self-assembling material from conventional coil-coil block copolymers because of the anisotropic arrangement of the conformationally rigid rod segments. To understand the self-assembly behavior and material properties in the rod-coil system, there have been extensive theoretical and experimental efforts.[1,2] Early theoretical works proposed that the coil volume fraction plays a crucial role in determining the assembled nanostructures.[3] It has

been also experimentally proven that the systematic variation of coil volume fraction manipulates a variety of supramolecular nanostructures from lamellar, continuous cubic to columnar morphologies.[4] As another independent variable for molecular rod assembly, we have investigated the influence of the rod length in triblock coil-rod-coil molecules, and demonstrated that larger anisotropy of the rod building block at a constant coil volume fraction leads to more continuous domain structures.[5] More recently, we have shown that molecular rods self-assemble into 2D continuous layers or discrete bundles depending on the coil cross-section, indicating that the cross-sectional area of the coil segments is also an important variable.[6]

The introduction of branched coil segments, e.g., star-like or dendritic coils into coil-coil block copolymers has been attempted to manipulate supramolecular structures.[7] The fusion of molecularly dissimilar blocks (i.e., linear and branched) causes different self-assembly behavior from that of linear coil block copolymers. Very recently, dendritic-linear hybrid block copolymers have been reported to show a unique morphological property, sharing the characteristics of the dendrimer and the linear block copolymer.[8] It has also been found that bearing more branched coil shifts the phase boundaries towards a larger volume fraction of the linear coil due to the interfacial curvature associated with coil branching.[9] However, such a molecular design concept to modulate self-assembled structures has been mostly limited to conformationally flexible coil-coil block copolymers.

A strategy to manipulate supramolecular structures assembled from rod segments may be accessible by the alteration of the coil architecture (linear versus branched) in the rod-coil system. A branched coil attached to a rod block would give rise to larger steric repulsions at the microphase separated rod/coil interface and, thus, lead to a discrete rod domain structure. We report here the fine tuning of 3D supramolecular crystalline structures from a perforated lamellar to a tetragonal micellar structure in a diblock rod-coil system by conforming to the above coil design concept (Figure 1). To this end, we have prepared two rod-coil molecules consisting of either a linear poly(propylene oxide) (PPO) coil or a dibranched PPO coil, respectively, both of which have the same coil volume fraction ($f = 0.84$), as a coil segment and a hexa-*p*-phenylene rod segment (Scheme 1). Thus, we can deduce that the supramolecular structural difference between the two molecules can be attributed to the coil architecture.

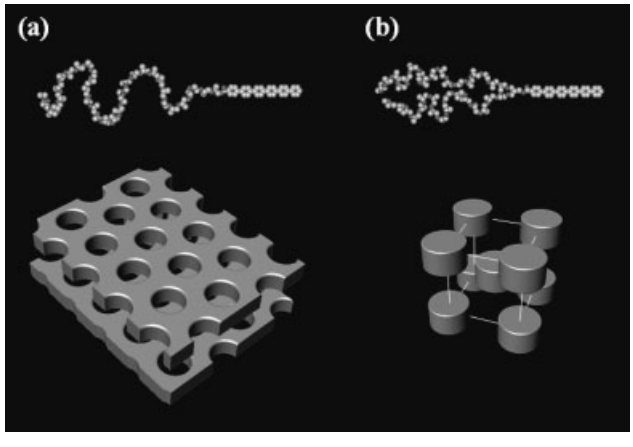

Figure 1. Schematic representation of 3D supramolecular structural change from (a) organized honeycombs to (b) organized bundles, dependent upon the coil architectural variation of the rod-coil molecule. For clarity, the lower schematics represent the structures consisting of rod segments.

Experimental Part

Materials

1,3-Diisopropylcarbodiimide (DIPC, 99%), 4-(dimethylamino)pyridine (DMAP, 99%), tetrakis(triphenylphosphine)palladium(0) (99%), iodine monochloride (1.0 M solution in dichloromethane), 4-bromobenzoic acid (all from Aldrich) and other conventional reagents were used as received. 4-trimethylsilyl-biphenyl-4′-boronic acid, 4-trimethylsilylbenzene boronic acid and 4-diphenylboronic acid were prepared according to previously described procedures.[10]

Synthesis

A general outline of the synthetic procedure used is shown in Scheme 1.

Synthesis of Rod-coil Molecules **6a** and **6b**

Compounds **6a** and **6b** were synthesized using the same procedure. A representative synthesis is described for **6a**. Compound **5a** (0.42 g, 0.16 mmol) and 4-diphenyl boronic acid (0.10 g, 0.50 mmol) were dissolved in degassed toluene (30 ml) and ethanol (2 ml). Degassed 2 M aqueous Na_2CO_3 (20 ml) was added to the solution and then tetrakis(triphenylphosphine)-palladium(0) (2.6 mg, 2.09 μmol) was added. The mixture was refluxed for 48 h with vigorous stirring under N_2. After cooling to room temperature, the layers were separated and the aqueous layer was washed twice with ethyl acetate. The combined organic layer was dried over anhydrous $MgSO_4$ and filtered. The solvent was removed in a rotary evaporator, and the crude products were purified by column chromatography (silica gel, ethyl acetate) to yield 0.38 g (87%) of a waxy solid with a melting point of 292 °C and a $\overline{M}_w/\overline{M}_n$ of 1.04 (GPC).

^{1}H NMR ($CDCl_3$): $\delta = 8.14$ (d, 2Ar-H, *o* to CH_2OOC, $J = 8.3$ Hz), 7.64–7.84 (m, 20Ar-H), 7.33–7.50 (m, 3Ar-H), 5.27–5.31 (m, 1H, $CH_2CH(CH_3)OOC$phenyl), 3.32–3.62 (m, 104H, OCH_3 and $OCH_2CH(CH_3)$), 1.02–1.34 (m, 102H, $CH(CH_3)O$).

6b was obtained in an 80% yield and had a melting point of 182 °C and a $\overline{M}_w/\overline{M}_n$ of 1.03 (GPC).

^{1}H NMR ($CDCl_3$): $\delta = 8.13$ (d, 2Ar-H, *o* to CH_2OOC, $J = 8.4$ Hz), 7.64–7.83 (m, 20Ar-H), 7.33–7.49 (m, 3Ar-H), 5.27–5.31 (m, 2H, phenylCOOCH_2CH), 3.49–3.62 (m, 112H, OCH_3 and OCH_2CH(CH_3)), 2.11 (m, 1H, $(CH_2)_2CHCH_2$), 1.02–1.34 (m, 102 H, $CH(CH_3)O$).

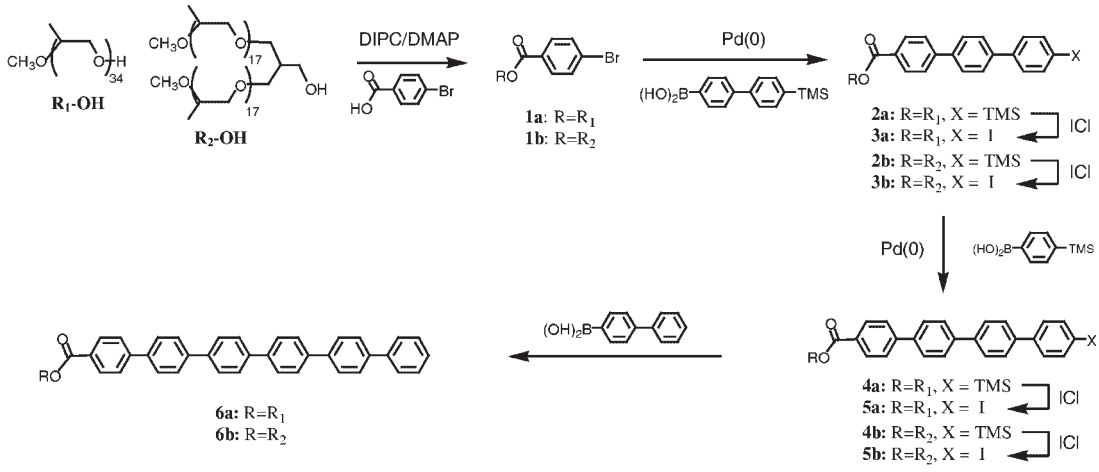

Scheme 1. Synthesis of rod-coil molecules **6a** and **6b**.

Characterization

^{1}H NMR and ^{13}C NMR spectra were recorded from $CDCl_3$ solutions on a Bruker AM 250 spectrometer. A Perkin Elmer DSC-7 differential scanning calorimeter equipped with a 1 020 thermal analysis controller was used to determine the thermal transitions. Molecular weight distributions were determined by gel permeation chromatography (GPC) with a Waters R401 instrument equipped with Styragel HR 3, 4 and 4E columns, a M7725i manual injector, a column heating chamber and a 2010 Millennium data station. X-ray scattering measurements were performed in transmission mode with synchrotron radiation at the 3C2 and 10C1 X-ray beam lines at Pohang Accelerator Laboratory, Korea. The transmission electron microscopy (TEM) experiments were performed at 120 kV using a JEOL 1020.

Results and Discussion

The synthetic procedure to obtain the rod-coil molecules is outlined in Scheme 1. It should be noted that the reason for the adoption of highly hydrophobic and anisotropic conjugated hexa-*p*-phenylene as a rigid rod block was to maximize the microphase separation between the rod and coil segments in the self-assembled structures. As mentioned earlier, the flexible coils were designed to be linear and dibranched PPOs which had identical molecular mass. The synthesis began with the preparation of the coil blocks. Linear PPO, **R_1-OH**, was purchased from Aldrich Corp. and used as received. Dibranched PPO, **R_2-OH**, was prepared through a combination of the Williamson etherification and hydroboration/oxidation reactions where the DP of the starting PPO was a half of **R_1-OH**.[11] 4-Bromobenzoic acid terminated coils **1a** and **1b** were synthesized by a diisopropylcarbodiimide mediated esterification reaction of the coils **R_1-OH** and **R_2-OH** with an excess amount of 4-bromobenzoic acid. They were then converted into trimethylsilyl-substituted triphenyl derivatives **2a** and **2b** using the Suzuki coupling reaction of 4-trimethylsilyl biphenyl-4′-boronic acid in the presence of Pd(0) catalyst.[12] For the next Suzuki coupling reaction, the trimethylsilyl group of **2a** and **2b** was substituted to the aryl iodide of **3a** and **3b** which is the most active in Suzuki-type aromatic couplings. Another subsequent iteration of the Suzuki coupling and iodization yielded **5a** and **5b**. Rod-coil molecules **6a** and **6b** with the hexa-*p*-phenylene rod segment were obtained by treating their corresponding precursor molecules **5a** and **5b** with aryl biphenyl boronic acid derivatives via a cross-coupling reaction. The purification of the resulting rod-coil molecules was performed by column chromatography (silica gel, ethyl acetate eluent) and sequential prep-HPLC. The rod-coil molecules were characterized by ^{1}H NMR spectroscopy and gel permeation chromatography (GPC). All of the analytical data was in full agreement with the presented structures. The rod-coil molecules had a narrow molecular weight distribution with a polydispersity index of less than 1.04.

Their thermal behavior was determined by differential scanning calorimetry (DSC). Both rod-coil molecules showed only a crystalline melting transition forming an isotropic liquid phase. Rod-coil molecule **6a** with the linear PPO coil showed a crystalline melting transition of rod segments at 292.2 °C on the heating scan. For rod-coil molecule **6b** with the dibranched PPO coil, however, a significant depression of the crystalline melting transition which occurred at 182.0 °C was observed. This may be attributed to the coil architectural change into the branched PPO because the dibranched coil has a larger coil cross sectional area which would hinder the regular packing of rod segments in the crystalline state. This argument can be corroborated by other supportive data from DSC and wide angle X-ray scattering (WAXS) investigations. From DSC data, the enthalpy change associated with the crystalline melting transition can be related to the relative

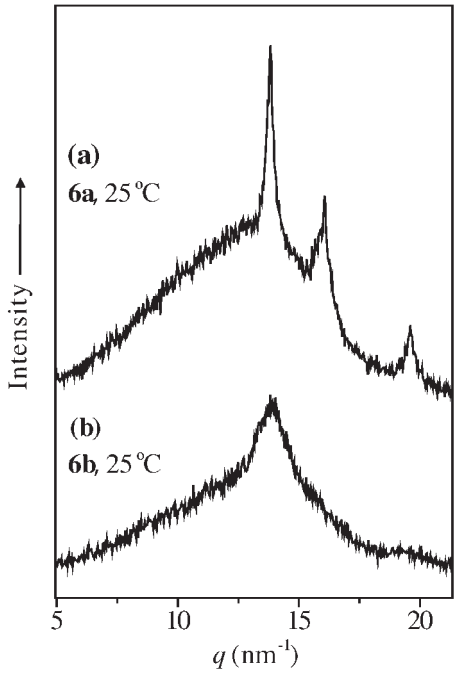

Figure 2. Wide angle X-ray diffraction patterns of (a) **6a** and (b) **6b** at 25 °C.

degree of rod packing. The heat of fusion (7.4 kJ · mol^{-1}) of **6a** was detected to be much larger than that of **6b** (3.9 kJ · mol^{-1}). This means that more energy is needed for the breakdown of the ordering of rod packing. Consistently, the WAXS data for **6a** showed a much sharper reflection pattern than that of **6b**, indicative of more ordered crystalline packing between the rod segments of **6a** (Figure 2).

To investigate the self-assembly behavior of the rod-coil molecules in their ordered state, small angle X-ray scattering (SAXS) and transmission electron microscopy (TEM) experiments were performed. In Figure 3(a), the SAXS pattern of **6a** shows a number of well-resolved reflections. These reflections can be indexed as a 3D hexagonal structure ($P6_3/mmc$ space group symmetry) with lattice parameters a = 13.4 nm and c = 18.8 nm. From the most intense (002) reflection, we can speculate that the fundamental structure is lamellar. For further analysis, the sample was cryomicrotomed to a thickness of ca. 50–70 nm and stained with RuO_4 vapor. Figure 3(c) shows a bright field TEM image. It reveals a regular array of bright domains with a hexagonal symmetry, surrounded by a dark matrix. From the density consideration, the image can be interpreted as light PPO coil domains which are hexagonally perforated in the dark rod layer. These results together with the SAXS data demonstrate that **6a** self-organizes into honeycomb-like crystalline layers of rods with in plane hexagonal packing of coil perforations, which are stacked in ABAB order.

In contrast, **6b** shows significantly distinct self-assembly behavior. In Figure 3(b), SAXS data for **6b** shows a sharp, low angle intense reflection and a number of sharp reflections of low intensity at higher angles. The observed reflections can be indexed as (110), (101), (002), (112) and (202) planes of a body-centered tetragonal lattice (space group $I4/mmm$) with lattice parameters a = 9.8 nm and b = 8.9 nm. Compared to the SAXS data for **6a**, the intensity of the (002) reflection in the SAXS data appears to be considerably weaker, suggesting that the basic structure consisting of more dense rod segments is micellar rather

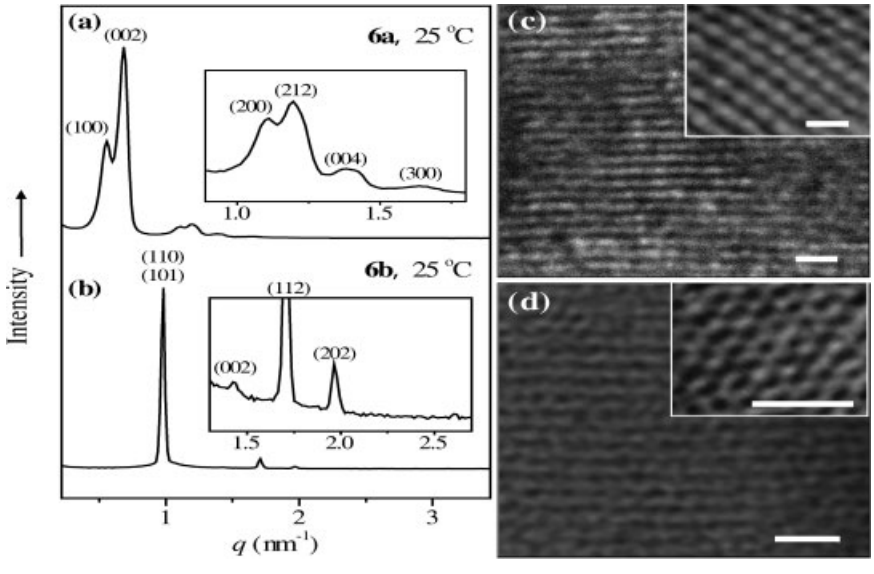

Figure 3. Small angle X-ray diffraction patterns of (a) **6a** and (b) **6b** at 25 °C, and TEM images (scale bar = 25 nm) of (c) a well-ordered layered microstructure of **6a** (inset: light-colored coil perforations in the dark aromatic matrix) and (d) the micellar microstructure of **6b** (inset: an ordered micellar array along the (111) direction).

than lamellar. To further corroborate the identity of the tetragonal micellar structure, a TEM image of a RuO_4 stained sample of **6b** was examined. In contrast to the TEM image of **6a**, dark rod domains were regularly arrayed in a light coil matrix (Figure 3(d)). On the basis of the SAXS and TEM results, we can conclude that **6a** self-assembles into discrete rod bundles of rods encapsulated by PPO coils, which are packed in a body centered tetragonal lattice.

The notable feature described here is that a simple structural variation from linear to dibranched chains generates a 3-dimensional supramolecular structural inversion from organized coil perforations in rod layers to organized discrete rod bundles in a coil matrix. The results demonstrate that the steric hindrance at the rod/coil interface arising from branched coils plays a crucial role in the self-assembly of rod segments as well as the conformational entropy associated with coil length.

Conclusion

Rod-coil molecules with identical coil volume fraction but different coil architectures, i.e., linear and dibranched, were synthesized and their self-assembling behavior in the solid state was investigated. On the basis of SAXS and TEM results, rod-coil molecules with a linear PPO coil showed a honeycomb-like lamellar rod assembly with hexagonally arrayed PPO coil perforations, while the rod-coil molecules with a dibranched PPO coil self-organized into rod-bundles with a body centered tetragonal symmetry surrounded by a PPO coil matrix. These results imply that the steric hindrance at the rod/coil interface is a dominant parameter governing supramolecular rod assembly in rod-coil systems.

Acknowledgements: This work was supported by the *National Creative Research Initiative Program of the Korean Ministry of Science and Technology*, the *Korea Science and Engineering Foundation* (R01–2006–000–11221–0), *Korea Research Foundation* (C00322) and *Seoul R&BD Program* (10668). We are grateful to *Pohang Accelerator Laboratory*, *Korea*(for use of the Synchrotron Radiation Source) and the *Brain Korea 21 program.*

[1] [1a] M. Lee, B.-K. Cho, W.-C. Zin, *Chem. Rev.* **2001**, *101*, 3869; [1b] M. Lee, Y.-S. Yoo, *J. Mater. Chem.* **2002**, *12*, 2161.

[2] [2a] J. T. Chen, E. L. Thomas, C. K. Ober, G.-P. Mao, *Science* **1996**, *273*, 343; [2b] S. I. Stupp, V. Lebonheur, K. Walker, L. S. Li, K. E. Huggins, M. Keser, A. Amstutz, *Science* **1997**, *276*, 384; [2c] E. R. Zubarev, M. U. Pralle, L. Li, S. I. Stupp, *Science* **1999**, *283*, 523; [2d] H.-A. Klok, J. F. Langenwalter, S. Lecommandoux, *Macromolecules* **2000**, *33*, 7819; [2e] S. A. Jenekhe, X. L. Chen, *Science* **1998**, *279*, 1903; [2f] G. Widawski, M. Rawiso, B. Francois, *Nature* **1994**, *369*, 387; [2g] S. Ludwigs, G. Krausch, G. Reiter, M. Losik, M. Antonietti, H. Schlaad, *Macromolecules* **2005**, *38*, 7532; [2h] H. Wang, H. H. Wang, V. S. Urban, K. C. Littrell, P. Thiyagarajan, L. Yu, *J. Am. Chem. Soc.* **2000**, *122*, 6855; [2i] M. A. Hempenius, B. M. W. Langeveld-Voss, J. A. E. H. van Haar, R. A. J. Janssen, S. S. Sheiko, J. P. Spatz, M. Möller, E. W. Meijer, *J. Am. Chem. Soc.* **1998**, *120*, 2798.

[3] [3a] A. N. Semenov, *Mol. Cryst. Liq. Cryst.* **1991**, *209*, 191; [3b] D. R. M. Williams, G. H. Fredrickson, *Macromolecules* **1992**, *25*, 3561.

[4] M. Lee, B.-K. Cho, H. Kim, J.-Y. Yoon, W.-C. Zin, *J. Am. Chem. Soc.* **1998**, *120*, 9168.

[5] B.-K. Cho, M. Lee, N.-K. Oh, W.-C. Zin, *J. Am. Chem. Soc.* **2001**, *123*, 9677.

[6] B.-K. Cho, Y.-W. Chung, M. Lee, *Macromolecules* **2005**, *38*, 10261.

[7] [7a] L. Yang, S. Hong, S. P. Gido, G. Velis, N. Hadjichristidis, *Macromolecules* **2001**, *34*, 9069; [7b] I. Gitsov, J. M. J. Fréchet, *Macromolecules* **1994**, *27*, 7309; [7c] M. E. Mackay, Y. Hong, M. Jeong, B. M. Tande, N. J. Wagner, S. Hong, S. P. Gido, R. Vestberg, C. J. Hawker, *Macromolecules* **2002**, *35*, 8391; [7d] J. C. M. van Hest, D. A. P. Delnoye, M. W. P. L. Baars, M. H. P. Van Genderen, E. W. Meijer, *Science* **1995**, *268*, 1592; [7e] J. Iyer, K. Fleming, P. T. Hammond, *Macromolecules* **1998**, *31*, 8757.

[8] B.-K. Cho, A. Jain, S. M. Gruner, U. Wiesner, *Science* **2004**, *305*, 1598.

[9] [9a] C. Román, H. R. Fischer, E. W. Meijer, *Macromolecules* **1999**, *32*, 5525; [9b] S. T. Milner, *Macromolecules* **1994**, *27*, 2333; [9c] F. L. Beyer, S. P. Gido, G. Velis, N. Hadjichristidis, N. B. Tan, *Macromolecules* **1999**, *32*, 6604.

[10] Y.-S. Yoo, J.-H. Choi, J.-H. Song, N.-K. Oh, W.-C. Zin, S. Park, T. Chang, M. Lee, *J. Am. Chem. Soc.* **2004**, *126*, 6294.

[11] [11a] J.-H. Ryu, N.-K. Oh, M. Lee, *Chem. Commun.* **2005**, 1770; [11b] J.-H. Ryu, J. Bae, M. Lee, *Macromolecules* **2005**, *38*, 2050.

[12] C.-J. Jang, J.-H. Ryu, J.-D. Lee, D. Sohn, M. Lee, *Chem. Mater.* **2004**, *16*, 4226.

